STUDIA UBB CHEMIA, LXX, 1, 2025 (p. 159-172)
(RECOMMENDED CITATION)
DOI:10.24193/subbchem.2025.1.11

GREEN SPECTROPHOTOMETRIC METHOD FOR CONCURRENT ESTIMATION OF PIROXICAM AND MEFENAMIC ACID MIXTURE

Fatma A. A. AL ANI[a], Azhar S. HAMODY[a], Ruaa M. MAHMOOD[a], Nahla A. ALASSAF[a], Dhafir T.A. AL-HEETIMI[a,*]

ABSTRACT. The purpose of this work is to concurrently estimate the UV-visible spectra of binary combinations of piroxicam and mefenamic acid using the chemometric approach. To create the model, spectral data from 73 samples (with wavelengths between 200 and 400 nm) were employed. A two-layer artificial neural network model was created, with two neurons in the output layer and fourteen neurons in the hidden layer. The model was trained to simulate the concentrations and spectra of piroxicam and mefenamic acid. For piroxicam and mefenamic acid, respectively, the Levenberg-Marquardt algorithm with feed-forward back-propagation learning produced root mean square errors of prediction of 0.1679 µg/mL and 0.1154 µg/mL, with coefficients of determination of 0.99730 and 0.99942, respectively. The suggested approach's ease of use, affordability, and environmental friendliness make it a suitable replacement for the use of hazardous chemicals in the routine investigation of the selected drugs.

Keywords: *piroxicam, mefenamic acid, concurrent estimation, artificial neural networks model*

INTRODUCTION

Nonsteroidal anti-inflammatory drugs, or NSAIDs, are among the most prescribed therapeutic agents. They can be used alone or in conjunction with other medications to treat a variety of clinical signs and symptoms, including both acute and chronic pain, as well as a variety of musculoskeletal disorders [1].

[a] *Department of Chemistry, College of Education for Pure Science/ Ibn Al-Haitham, University of Baghdad, Baghdad-Iraq.*
[*] *Corresponding author: dhafir.t.a@ihcoedu.uobaghdad.edu.iq, dhafir1973@gmail.com*

In 1982, piroxicam was first made available as Feldene in the United States, where it was quickly accepted [2]. It is used to treat acute gout and to relieve the symptoms of rheumatoid arthritis, osteoarthritis, and both in short- and long-term therapy [3]. One derivative of anthranilic acid is mefenamic acid [4]. Although it has some mild anti-inflammatory activity, its principal use since its introduction to the United States in 1967 has been pain relief [2]. Mefenamic acid inhibits both the generation of prostaglandins and the tissue's reaction to them. It is mostly eliminated in the urine and is strongly attached to plasma proteins [5]. Figure 1 displays the mefenamic acid and piroxicam structural formulas [6].

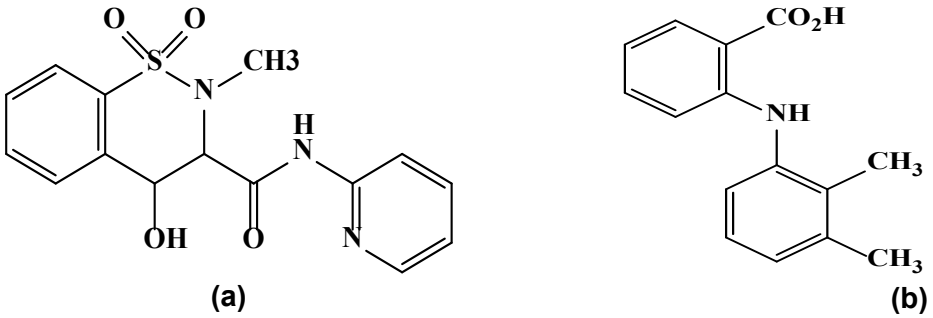

Figure 1. Structures formula of (a) piroxicam and (b) mefenamic acid

A review of the literature reveals several standard analytical methods for the simultaneous or individual quantification of pharmaceutical formulations, bodily fluids, and the pharmaceuticals under study in bulk. Spectrophotometry [7–9], potentiometry [10–11], GC-Mass [12–13], flow injection analysis [14,15], and HPLC [16-18] are a few of these techniques.

For quantitative pharmaceutical analysis, spectrophotometry in conjunction with chemometric methods like artificial neural networks (ANNs) is the most practical, cost-effective, and adaptable analytical approach [19]. As far as we are aware, no report has utilised this technique (ANNs) to determine piroxicam and mefenamic acid together.

The primary objective of this study is to broaden the application of chemometric techniques, such as artificial neural networks (ANNs), for the simultaneous prediction of mefenamic acid and piroxicam in their binary synthetic mixes. ANNs are well-suited to model the nonlinear relationships between variables. This making them effective for analyzing complex chemical

data where traditional linear methods might fall short. ANNs learn from data, meaning they can be trained on a dataset of known spectra and concentrations to develop a model that can predict the concentrations of piroxicam and mefenamic acid in unknown samples. This data-driven approach allows for high accuracy and adaptability. Once trained, ANNs can quickly and accurately analyze new samples without the need for extensive manual intervention. This makes the method highly efficient for routine analysis in laboratories. Finally, ANNs can handle noisy and incomplete data better than many traditional methods. This robustness is particularly valuable in chemical analysis, where experimental data can often be imperfect.

The primary distinction between the current green investigation and the earlier published work is the simultaneous determination of both forms without the need for laborious stages like species masking or separation, minimizes waste generation by using UV spectra, and in addition, the ANN method performed at ambient temperature and pressure, reducing energy consumption.

RESULTS AND DISCUSSION

Having overlapped spectral features makes it difficult to distinguish between different species when conducting spectrophotometric studies of them in combination. An ANN model made it feasible to conduct these kinds of investigations, where there is a great deal of overlap in the responses of the components under study [19].

Figure 2 represents the absorption spectra of piroxicam and mefenamic acid as well as their mixture which show a strong spectral overlap. To overcome this problem, the ANN method was proposed, which was associated with spectrophotometry.

To build up the ANN model, spectral data of 73 synthetic binary mixture at various piroxicam concentrations (1.0–13.0 µg/mL) and mefenamic acid (1.0–18.0 µg/mL) were used (Figure 3). This range of concentration is adopted to ensure that the absorption value of the mixture is kept within the limits preferred in Bierre Lambert's law, namely (1.5-2.0). These spectra were recorded in wavelength range of (200–400) nm to improve, standardize, and validate the recommended model. In this method, there is no optimal wavelength to measure, but the entire absorption spectrum is taken to describe the concentration in question.

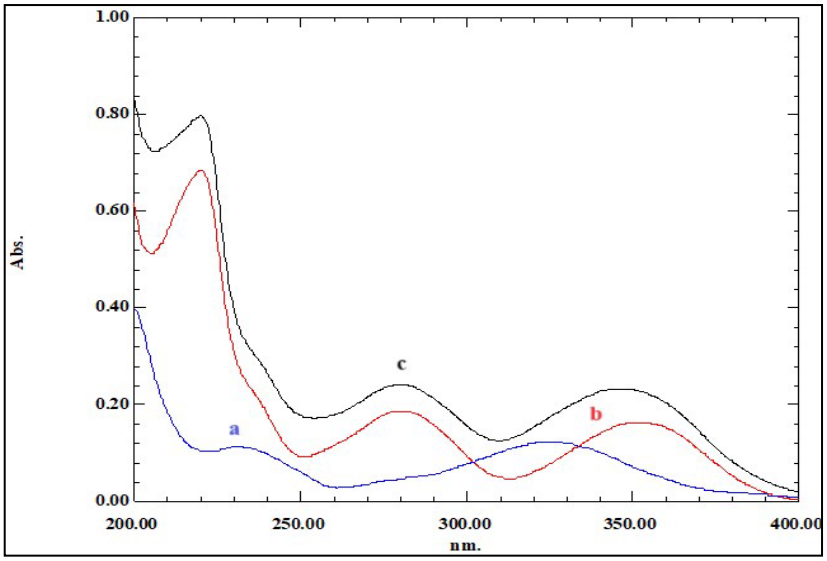

Figure 2. Absorption spectra of (a) 2µg/mL piroxicam (b) 6µg/mL mefenamic acid and (c) mixture of 2µg/mL piroxicam and 6µg/mL mefenamic acid, all of it against methanol as a blank solution

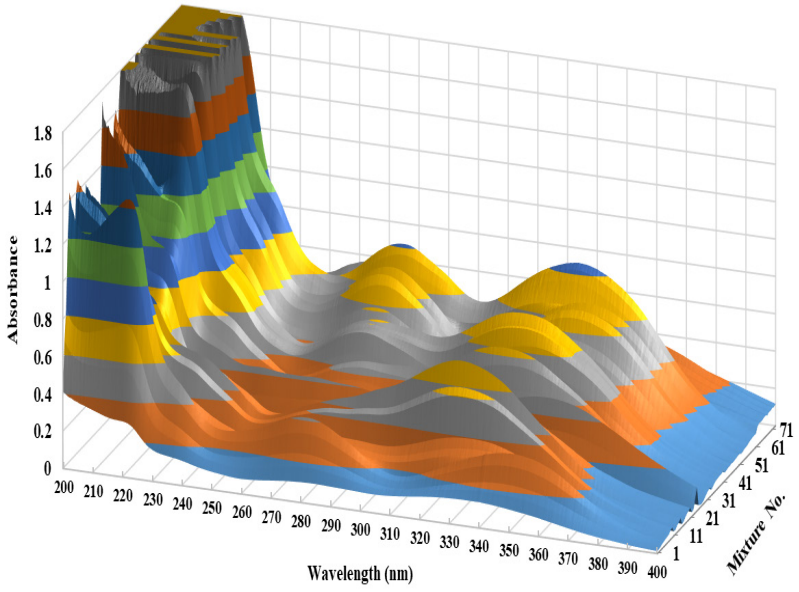

Figure 3. Three-dimensional absorbance spectra of 73 mixtures of piroxicam (1.0-13.0 µg/mL) and mefenamic acid (1.0-18.0µg/mL) against methanol as a blank solution

In order to model the concentrations of piroxicam and mefenamic acid, the spectral data matrix of their mixtures, which included the absorbance of 73 mixture, was added as an input data, and the experimental concentrations of both drugs were added to the network toolbox separately as target matrices. This is because the ANN construction is a crucial parameter to determine the performance of the model. The total number of inputs was 2002, with 1001 inputs for absorption and 1001 inputs for wavelengths. The wavelength increased in increments of 0.2 nm, ranging from 200 nm to 400 nm.

A multi-layered neural network with Levenberg–Marquardt training algorithm for its quick merging was established. A MATLAB program for a two-layered artificial neural network was created. This model has two input vectors (wavelengths and absorbances), two output vectors (concentration of piroxicam and mefenamic acid), and fourteen neurones in the hidden layer. Figure 4 shows the created neural network and its training techniques as well as its performance over time.

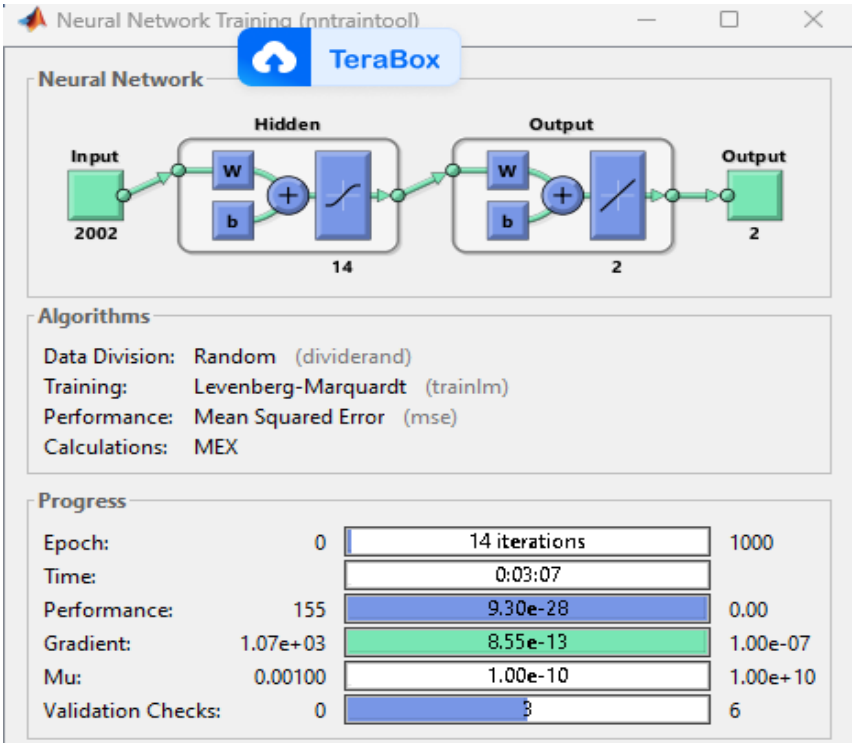

Figure 4. Architecture of the proposed ANN used for training the experimental spectral data

In accordance with standard protocol for ANN model training, seventy percent of the data were allocated to network training (51 mixture), fifteen percent were used for network validation (11 mixture), and the remaining fifteen percent were fed into the network (11 mixture) as test data to gauge the model's predictive capacity. Figure 5 shows the performance of the model over multiple epochs. An epoch refers to one complete pass through the entire training dataset. During an epoch, the model processes each example in the training set once, and the model's parameters (weights and biases) are updated based on the errors made during this pass. Highlighting the point at which the model achieved its best validation performance is crucial for understanding the model's learning process and determining the optimal number of epochs for training. "Best Validation Performance is 0.49767 at epoch 11," indicating that the lowest validation error was achieved at epoch 11 with a value of 0.49767.

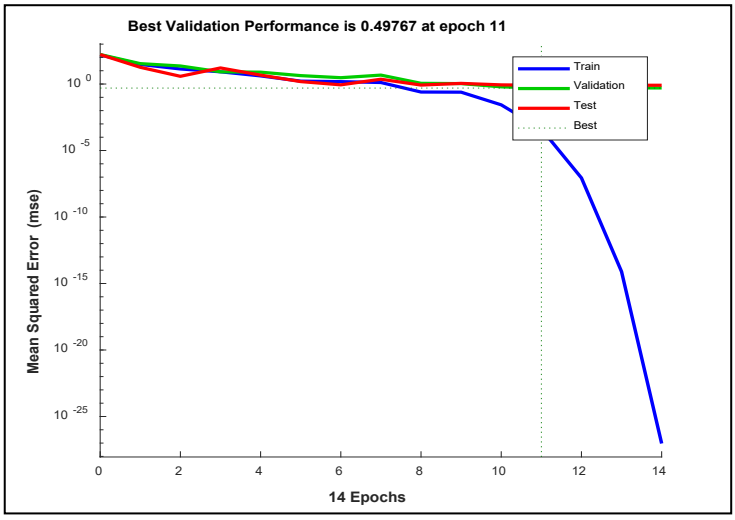

Figure 5. The training 14 epoch versus mean square error (mse)

As seen in Figure 6, the predicted and actual concentrations of mefenamic acid and piroxicam are plotted. Better predictions from both components are supported by higher values of the coefficient of determination (R) for training, validation, and testing. Rejecting and retraining any findings that are not satisfactory is a crucial step in the computation mode.

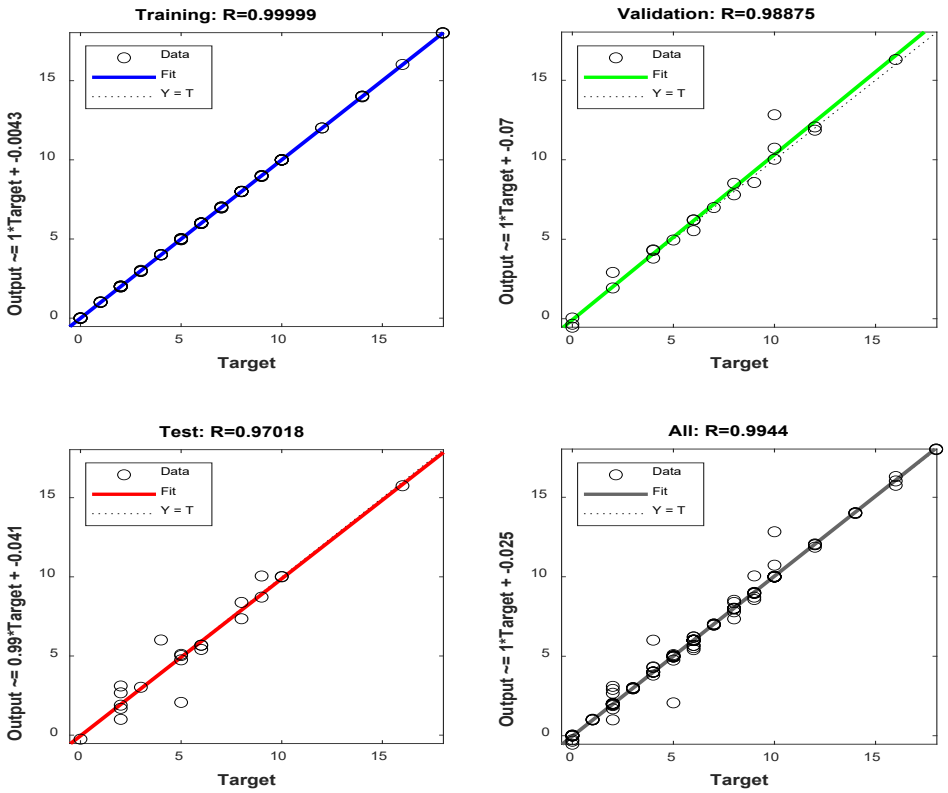

Figure 6. Actual concentrations versus the predicted concentrations and R values for training, validation, and testing series of the proposed ANN model

Following model fine-tuning, the ANN's training phase was carried out independently for each component using Levenberg-Marquardt techniques for error minimisation. Table 1 shows the RMSE and R^2 for each component at each step.

Table 1. The performance parameters of the proposed ANN model

Data	No. of Samples	Mefenamic acid		Piroxicam	
		RMSE (µg/mL)	**R^2**	**RMSE (µg/mL)**	**R^2**
Training	51	0.09903585	0.999324	0.17661867	0.997241
Validation	11	0.10195360	0.999602	0.08162060	0.999648
Testing	11	0.09854842	0.999512	0.21328921	0.993747

The following formulas are used to compute the coefficient of determination (R^2) and root mean square error (RMSE) [20]:

$$RMSE = \sqrt{\frac{\sum_{i=1}^{N}(\hat{y}_i - y_i)^2}{N}}$$

$$R^2 = 1 - \frac{\sum_{i=1}^{N}(\hat{y}_i - y_i)^2}{\sum_{i=1}^{N}(\acute{y}_i - y_i)^2}$$, where:

$\hat{y}_i$ predicted concentration in the ith sample,
y_i actual value for the sample concentration,
$\acute{y}_i$ mean of the actual values,
N number of samples in validation group.

After retraining, the data evaluated in the model indicated about 100% fitting, which is indicative of the conformation of the ANN model. Figures 7 and 8 show the plotted architecture of the ANN model. The blue line represents the taken concentration (µg/mL) that was supposed to be present in each sample while the red line represents the predicted (found) concentration (µg/mL) detected in each sample through analysis. The closer the red line is to the blue line, the more accurate the detection method is. By examining the trends in the graph, we can identify patterns or anomalies in the detection process.

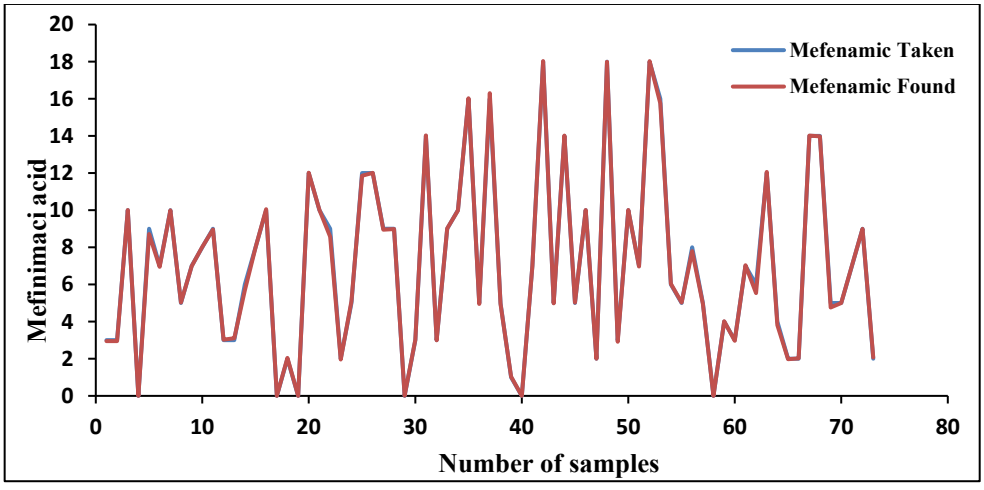

Figure 7. ANN model for Mefenamic acid

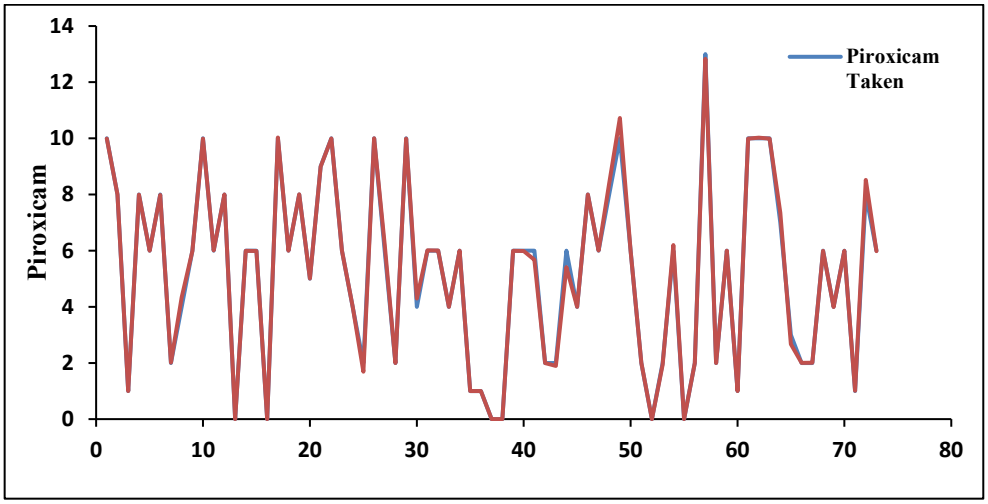

Figure 8. ANN model for Piroxicam

Figure 9 represent the error distribution where the majority of errors are centred around zero, indicating that the model's predictions are generally close to the actual target values. The blue bars represent the errors for the training dataset. Most of these errors are clustered around zero, with a few instances showing larger errors. This indicates that the model has learned well from the training data. The green bars represent the errors for the validation dataset. These errors are also mostly centred around zero, but there are some instances with larger errors. This suggests that the model is generalizing well to new data, but there is still room for improvement. The red bars represent the errors for the test dataset. Similar to the validation dataset, the errors are mostly centred around zero, with a few larger errors. This indicates that the model's performance on unseen data is consistent with its performance on the validation data. The orange line represents zero error, serving as a reference point. The closer the bars are to this line, the better the model's predictions. The ANN model's display of the error histogram indicates random variation in the absence of systematic error.

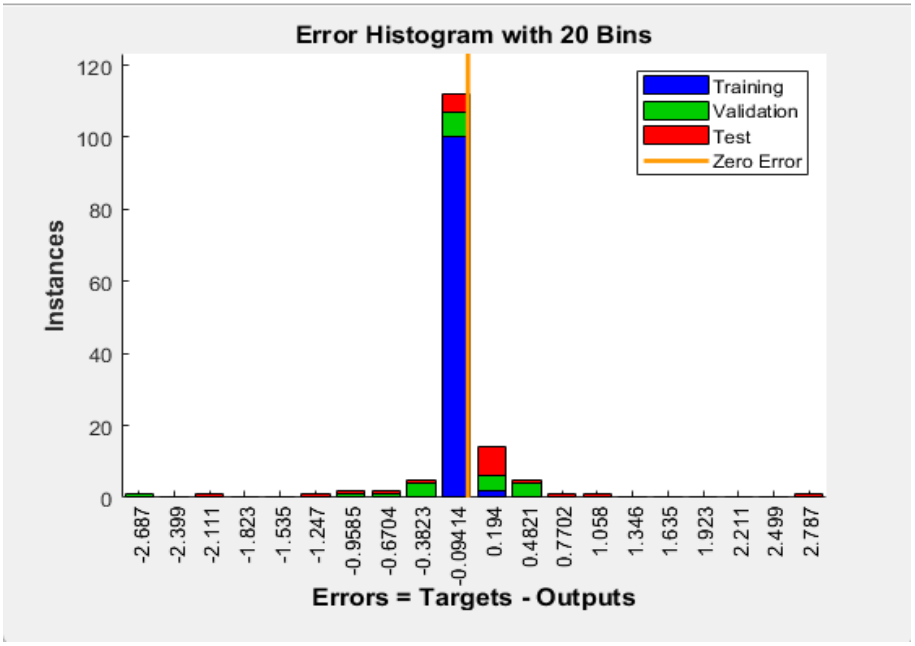

Figure 9. Error histogram for ANN model

The performance of the proposed method is also evaluated using the percentage recovery values (Rec%) of the concentrations of both mefenamic acid and piroxicam. Results of Rec% in Table 2 show the successful applicability of ANN model for concurrent estimation of both components in their mixture.

Table 2. Recoveries of mefenamic acid and piroxicam in 11 test samples by the ANN model

Mixture No.	Mefenamic acid			Piroxicam		
	Taken (µg/mL)	Found (µg/mL)	Rec%	Taken (µg/mL)	Found (µg/mL)	Rec%
1	18	18.033	100.18	10	9.991	99.91
2	10	10.013	100.13	6	5.984	99.73
3	12	12.020	100.17	13	12.831	98.70
4	14	14.025	100.18	2	2.003	100.15
5	16	16.027	100.17	2	2.010	100.50
6	18	18.033	100.18	6	5.995	99.92
7	10	9.984	99.84	4	3.994	99.85
8	12	11.859	98.83	6	5.993	99.88
9	14	13.975	99.82	1	1.011	101.10
10	18	17.994	99.97	10	10.023	100.23
11	16	15.754	98.46	6	5.984	99.73

Using Anova: Single Factor, the findings of the suggested ANN model for each drug were statistically compared with those of the created RP-HPLC method [16] in term of recoveries of the found concentration from calibration graphs (Figure 6) and PLS calibration model [9] in term of recoveries of the predicted concentration of validation set (Figure 6, A and D). The results of Table 3 show that there is a statistically significant difference between the means of the three groups, as indicated by a higher F statistic value (7.67608, 7.66838 for mefenamic acid and piroxicam, respectively) and a p-value less than α =.05. Therefore, the null hypothesis of the ANOVA is rejected. Based on the summary statistics and ANOVA results, the ANN method appears to be the best for estimating mefenamic acid and piroxicam, as it has the highest average and the lowest variance, indicating more accurate and consistent results.

Table 3. An summary of the one-way ANOVA comparison between the reported methods (HPLC method and PLS model) and the proposed ANN model

Summary Statistics of **Mefenamic acid** *estimation*						
Method	***Count***		***Sum***		***Average***	***Variance***
PLS	10		992.9867		99.2987	2.86314
HPLC	10		978.9289		97.8929	1.66270
ANN	10		1000.5516		100.0552	0.17965
ANOVA						
Source of Variation	***SS***	***df***	***MS***	***F***	***P-value***	***F crit***
Between Groups	24.0797	2	12.03987	7.67608	0.00229	3.35413
Within Groups	42.3493	27	1.56849			
Summary Statistics of **Piroxicam** *estimation*						
Method	***Count***		***Sum***		***Average***	***Variance***
PLS	10		995.2936		99.5294	1.00113
HPLC	10		981.7495		98.1746	2.15856
ANN	10		1000.0700		100.0070	0.37511
ANOVA						
Source of Variation	***SS***	***df***	***MS***	***F***	***P-value***	***F crit***
Between Groups	18.07078	2	9.03539	7.66838	0.00231	3.35413
Within Groups	31.81320	27	1.17827			

- *Null hypothesis: The means of all selected datasets are equal.*
- *Alternative hypothesis: The means of one or more selected datasets are different.*
- *At the 0.05 level, the population means are not significantly different.*

CONCLUSION

Because of spectrum overlap, it might be difficult to accurately determine the concentration of two species at the same time using traditional spectroscopy. In many domains, chemometric and machine learning algorithms are increasingly widely used, but they are particularly well-liked in multivariate spectroscopic investigation of complicated mixtures. The relationship between UV spectra and the simultaneous levels of piroxicam and mefenamic acid was modelled using an artificial neural network.

In addition to having low mean square error values for prediction, the constructed ANN model also has a high determination coefficient from the model's external validation and adequate recovery values, which make it capable of resilient concurrent analysis.

EXPERIMENTAL

Apparatus

Shimadzu 1800 UV-vis spectrophotometer, equipped with 1 cm quartz cells with UV Prob 2.34 software included, was used to accomplish all of the absorption spectra. The 200–400 nm wavelength range, 0.2 nm data interval, medium scan rate, single scan mode, and 1.0 mm slit width were all used for the scans. Every sample was scanned three times, and its representation was derived from the average of three spectra. No pre-processing was done on the spectral data.

Software

A Simplex Lattice Mixture Design, developed by JMP® 11.0.0 SAS Institute Inc., was utilised to generate a series of calibration mixtures for the simultaneous measurement of piroxicam and mefenamic.

Chemicals and reagents

The State Company for Drug Industries and Medical Appliances Samara-Iraq (SDI) provided the piroxicam and mefenamic acid raw powders utilised in this investigation, which had a purity of 99.99%. The methanol used in this study was an analytical grade reagent.

Standard and working solutions

Mefenamic acid and piroxicam standard stock solutions (1000 µg/mL) were made individually by dissolving 0.050 g of each medication in 50 mL methanol. Working solutions were prepared as needed by the process of serial dilution.

Data analysis

MATLAB (version 9.1.0 R2021a, Math Work, Inc) was used for obtaining the analysed data.

ACKNOWLEDGEMENT

I express my sincere gratitude to Ass. Prof. Saad Ali Ahmed for his efforts in creating the artificial neural network model that served as the basis for this investigation. His help was invaluable in expediting the decision-making process and enabling the analysis performed for this study.

REFERENCES

1. R. Brennan; M. Wazaify; H. Shawabkeh; I. Boardley; J. McVeigh; M.C.Van Hout; *Drug Saf.*, **2021**, *44*,917-928.
2. V. F. Roche; S. W. Zito; T. L. Lemke; D. A. Williams; *Foye's principles of medicinal chemistry*, 8th ed.; Lippincott Williams & Wilkins, **2019**, p.1018.
3. V. Alagarsamy; *Textbook of medicinal chemistry*, Elsevier Health Sciences, 2, **2010**, p.92.
4. J. K. Aronson; *Meyler's side effects of analgesics and anti-inflammatory drugs*; Elsevier, **2009**, p.310.
5. H. Benzon; S. N. Raja; S. M. Fishman; S. Liu; S. P. Cohen; *Essentials of pain medicine*, 3rd ed.; Elsevier Health Sciences, **2011**, p.135.
6. *British Pharmacopoeia*, London, UK, **2022**, volume II, 217, 648.
7. S. Singh; J. R. Patel; S. Kare; *Asian J. Res. Chem.,* **2016**, *9(2)*, 82-84.
8. H. Wasit; D. Purnamasar; M. S. Fareza; *Malaysian J. Anal. Sci.,* **2021**, *25(1)*,71-80.
9. R. M. Mahmood; S. A. Darweesh; N. A. Alassaf; R. S. Al-Khalisy; *Methods Objects Chem. Anal.,* **2024**,*19(2)*, 101-110.
10. N. Rajendraprasad; K. Basavaiah; *Curr. Chem. Lett.,* **2016**, *5(1)*, 33-46.
11. Z. A. Kormosh; O. Y. Matviichuk; I. P. Antal; Y. R. Bazel; *J. Anal. Chem.*, **2020**, *75(6)*, 820-828.

12. A. Krokos; E. Tsakelidou; E. Michopoulou; N. Raikos; G. Theodoridis; H. Gika; *Separations*, **2018**, 5, 37.
13. B.M. El Haj; A.M. Al Ainri; M.H. Hassan; R.K. Bin Khadem; M.S. Marzouq; *Forensic Sci. Int.,* **1999**, *105*, 141–153.
14. R. I. Abed; H. Hadi; *Bull. Chem. Soc. Ethiop.,* **2020**, *34(1),*13-23.
15. L. Al-Ameer; K. K. Hashim; D. N. Taha; *Water Pract. Technol.,* **2022**, *17(9)*,1881-1892.
16. S. B. Dikran; R. M.Mahmood; *J. Univ. Babylon Pure Appl. Sci.*, **2018**, *26(5)*, 387-399.
17. M. Celebier; M. Nenni; O. Kaplan; E. Akgeyik; M. S. Kaynak; S. Şahİn; *Turkish J. Pharm. Sci.,* **2020**, *17(5)*, 535-541.
18. V.N.K. Kopparapu; P. Kasula; A.K.R. Ankinapalli; M. Venkateswarlu; *International Journal of Pharmaceutical Quality Assurance,* **2019**,*10(4)*, 583-587.
19. A.S. Hamody; F.H. Zankanah; S.A. Ali; N. Alassaf; S.B. Dikran; *Methods Objects Chem. Anal.,* **2022**, *17(3)*, 118-124.
20. Y. Nausheen; S. M. Naqvi; S. M. Akhter; *Heliyon*, **2024**,*10(4)*, 2024, e26373,